Title 論文題目	An Intronic Single Nucleotide Polymorphism in the *MUTYH* Gene Is Associated with Increased Risk for HCV-induced Hepatocellular carcinoma （MUTYH 遺伝子のイントロン一塩基多型は HCV 誘発性 HCC 発癌リスクの上昇と関連する）
Author(s) 著　者	櫻田，晃
Degree number 学位記番号	甲第 2949 号
Degree name 学位の種別	博士（医学）
Issue Date 学位取得年月日	2017-03-31
Original Article 原著論文	札幌医学雑誌第 86 巻第 1 号
Doc URL	
DOI	
Resource Version	

学位申請論文

An Intronic Single Nucleotide Polymorphism in the *MUTYH* Gene Is Associated

with Increased Risk for HCV-induced Hepatocellular carcinoma

腫瘍内科学講座

櫻田　晃

An Intronic Single Nucleotide Polymorphism in the *MUTYH* Gene Is Associated with Increased Risk for HCV-induced Hepatocellular carcinoma

Short Title: A SNP in the *MUTYH* Associated with Risk for HCC

AKIRA SAKURADA,[1] KOJI MIYANISHI,[1,#] SHINGO TANAKA,[1] MASANORI SATO,[1] HIROKI SAKAMOTO,[1] YUTAKA KAWANO,[1] KOHICHI TAKADA,[1] YUSAKU NAKABEPPU,[2,#] MASAYOSHI KOBUNE,[1] and JUNJI KATO[1,#]

[1] Department of Medical Oncology, Sapporo Medical University School of Medicine, Sapporo, Japan

[2] Division of Neurofunctional Genomics, Department of Immunobiology and Neuroscience, Medical Institute of Bioregulation, Kyushu University, Fukuoka, Japan

[#] Corresponding authors.

Grant Supports: This work was supported by JSPS KAKENHI Grant Numbers JP24590985, JP19390202, JP17390220.

Abbreviations used in this paper: ROS, reactive oxygen species; 8-oxodGuo, 8-oxo-7,8-dihydro-2'-deoxyguanosine; 8-oxoguanine or GO, 8-oxo-7,8-dihydroguanine; OGG1, 8-oxoguanine DNA glycosylase protein; CI, confidence interval; HR, hzard ratio; SNP, single nucleotide polymorphism

Correspondence: Koji Miyanishi, M.D., Ph.D., Department of Medical Oncology, Sapporo Medical University, School of Medicine, South-1, West-16, Chuo-ku, Sapporo, 060-8543,

Japan.

TEL: (+81)-11-611-2111(ext.3260); FAX:(+81)-11-612-7987

e-mail: miyako@sapmed.ac.jp

or Junji Kato, M.D., Ph.D, Department of Medical Oncology, Sapporo Medical University School of Medicine, South-1, West-16, Chuo-ku, Sapporo, 060-8543, Japan.

TEL: (+81)-11-611-2111(ext.3260); FAX:(+81)-11-612-7987

e-mail: jkato@sapmed.ac.jp

or Yusaku Nakabeppu, Ph.D, Division of Neurofunctional Genomics, Department of Immunobiology and Neuroscience, Medical Institute of Bioregulation, Kyushu University, 3-1-1 Maidashi, Higashi-Ku, Fukuoka 812-8582, Japan.

TEL: (+81)-92-642-6814; FAX:(+81)-92-642-6246

yusaku@bioreg.kyushu-u.ac.jp

Disclosures: The authors have nothing to disclose.

Author contributions: A.S., K.M. and S.T. performed most of the experiments, analyzed and interpreted the data. Y.K., K.T. and M.K. provided logistical support and discussed the data. M.S. and H.S. provided support with experimental materials and techniques. K.M., J.K. and Y.N designed and directed the overall project, and wrote the manuscript.

Acknowledgements: This work was partly performed in the Cooperative Research Project Program of the Medical Institute of Bioregulation, Kyushu University.

Abstract

BACKGROUND & AIMS: The role of base excision repair genes in human hepatocarcinogenesis has not yet been explored. Here, we investigated relationships between variants of these genes and the risk of developing hepatocellular carcinoma (HCC).

METHODS: Nineteen tagging SNPs in base excision repair genes (including *MUTYH*, *OGG1* and *MTH1*) were genotyped using iPLEX assays; one significant SNP was found and confirmed in Japanese patients with chronic hepatitis C (CHC) (n=38 HCC and 55 controls). The effects of modifying the intronic variants were determined by luciferase assays. MUTYH-null mice were used to examine the involvement of oxidative stress and DNA repair enzymes in hepatocarcinogenesis.

RESULTS: Significant associations were found for a single intron SNP (rs3219487) in the *MUTYH* gene. The risk of developing HCC in patients with A/A or G/A genotypes was higher than in those with the G/G genotype (OR=9.27, 95% CI=2.39–32.1, P=0.0005). *MUTYH* mRNA levels in both peripheral mononuclear cells and liver tissues were significantly lower in G/A or A/A genotyped subjects (P=0.0157 and 0.0108, respectively). We found that -2000 in the *MUTYH* promoter region is involved in enhanced expression of *MUTYH* by insertion of a major allele sequence of rs3219487. Liver tumors were observed in MUTYH-null mice after 12 months´ high iron diet, but no tumors developed when dietary anti-oxidant (N-Acetyl-L-cysteine) was also provided.

CONCLUSIONS: CHC patients with the rs3219487 adenine allele had a significantly increased risk of developing HCC. MUTYH-null mice with iron-associated oxidative stress were susceptible to development of liver tumors unless prevented by dietary anti-oxidants.

Keywords: ROS; liver cancer; iron; NAC

Introduction

Hepatitis C virus (HCV) is a major cause of chronic hepatitis, liver cirrhosis, and hepatocellular carcinoma (HCC). Follow-up studies on the natural history of chronic hepatitis C (CHC) over a mean period of 4-11 years have shown that cirrhosis develops in 8-46% of cases and HCC in 11-19%[1-3]. Recent studies have shown that excess hepatic iron accumulation in CHC patients contributes to liver injury[4-6]. It is believed that free iron in the liver facilitates the formation of reactive oxygen species (ROS), including hydroxyl radicals (·OH), which cause oxidative damage to numerous cellular components, including lipids, proteins and nucleic acids, and also cause increased collagen synthesis[7]. Further, ·OH is known to generate promutagenic bases such as 8-oxo-7,8-dihydro-2'-deoxyguanosine (8-oxodGuo), which is highly mutagenic because it mispairs with cytosine and adenine with an almost equal efficiency during DNA replication. This leads to an increased frequency of G:C to T:A transversions that can lead to carcinogenesis when occurring in oncogenes or tumor suppressor genes[8,9]. Because the liver is an iron-rich organ containing ~30% of the total amount of iron stored in the body[10], it is considered to be one of the most susceptible to cellular damage or DNA mutagenesis caused by ROS. In this regard, we have shown previously that in Long-Evans cinnamon rats, an acute accumulation of iron in the liver causes spontaneous hepatitis and subsequent development of HCC[11]. It is therefore plausible that ROS and iron are involved in the hepatocarcinogenesis of HCV infection in humans. There have, in fact, been reports demonstrating that there is an accumulation of 8-oxodGuo in the livers of patients with chronic hepatitis C and HCV-related HCC[12,13]. In a 6-year follow-up study of CHC patients, we previously demonstrated that iron depletion therapy, consisting of intermittent phlebotomies and a low-iron diet, significantly reduced serum ALT levels, the histological hepatic fibrosis grade, and hepatic 8-oxodGuo levels[6]. Further, we also demonstrated that continuation of iron

depletion therapy for CHC can decrease the incidence of progression to HCC[14].

Base excision repair is the important cellular mechanism for removal of 8-oxo-7,8-dihydroguanine (8-oxoguanine or GO). Human MutY homolog (MUTYH) protein is responsible for recognition and removal of the inappropriately inserted adenine opposite GO[13] and the OGG1 protein, which has 8-oxoguanine DNA glycosylase activity, removes the mutagenic GO lesion and other oxidized purines incorporated opposite cytosines[15,16]. MutT homolog-1 (MTH1) suppresses the accumulation of 8-oxodGuo by hydrolysis of oxidized purine nucleotides accumulated in the nucleotide pool[17-19]. Some studies have described a possible role of variants of these genes as risk modifiers in different types of cancer such as colon, head and neck, lung or kidney[15,16,20]. However, the role of variants of these genes in human hepatocarcinogenesis has not yet been explored. Here, we investigated whether there is a causative relation between variants of these genes and the risk for HCV-induced HCC. Furthermore, we examined the involvement of oxidative stress and DNA repair enzymes in hepatocarcinogenesis using a murine model.

Materials and Methods

Study population

Patients diagnosed as having CHC at our Department between 2007 and 2015 were enrolled. All were of Japanese origin, provided written informed consent, and routinely visited the Liver Unit. They met the following criteria: (a) ≥45 years of age with detectable anti-HCV antibodies and HCV-RNA; (b) histopathological evidence of chronic hepatitis on liver biopsy; (c) negative test result for anti-nuclear antibody, anti-smooth muscle antibody, anti-mitochondrial antibody, or hepatitis B surface antigen; and (d) no habitual drug or alcohol use. This study was approved by the Ethics Committee of our University.

For the present study, a first phase exploratory cohort and a second phase

confirmatory cohort were defined. The exploratory cohort consisted of 40 patients with CHC who met the above inclusion and exclusion criteria. The confirmatory cohort comprised all patients of the exploratory cohort, and additional patients with CHC who also met the inclusion and exclusion criteria (total n=93). In both the exploratory and confirmatory cohorts, patients with proven HCC are designated "cases", whereas patients with no diagnosis of HCC up to the date of analyses are designated "controls".

Clinical information such as age, gender, smoking history, alanine aminotransferase (ALT), gamma-glutamyl transpeptidase (GGT) and platelet count was available for all subjects. For cases, age, ALT, GGT and platelet count at initial diagnosis of HCC were used. Diagnostic criteria of HCC were as follows: (a) histological confirmation; or (b) two different liver imaging examinations showing a lesion with typical characteristics of HCC (hypervascular nodule, intrahepatic multiplicity and pathognomonic findings of capsule formation or nodule-in-nodule appearance or even portal vein invasion). In addition, in the subgroup of patients with a known duration of CHC since diagnosis, uni- and multivariable Cox regression analyses were performed to assess the time from CHC diagnosis to the date when HCC was diagnosed for the first time.

SNP Selection and Genotyping

In the exploratory cohort, Tag SNPs for each base excision repair gene (*MUTYH*, *OGG1* and *MTH1*) were selected using the SNP Annotation and Proxy Search (SNAP) program ver.2.2[21] based on the CHBJPT panel of 1000 genomes Project Pilot 1[22] using the following criteria: minor allele frequency (MAF) >0.1, pairwise r^2>0.8 and distance limit 500 kb.

Genomic DNA was extracted from peripheral mononuclear cells using the DNeasy Blood & Tissue Kit (QIAGEN GmbH, Hilden, Germany). The SNP genotyping was performed

by Agena MassARRAY platform with iPLEX gold chemistry (Agena, San Diego, CA) according to the manufacturer's instructions[23]. The specific PCR primer and extension primer sequences were designed using the Assay Designer software package (v.4.0). The purified primer extension reaction was loaded onto a matrix pad of a SpectroCHIP (Agena) and then analyzed using a MassARRAY Analyzer 4 (Sequenom, Inc., San Diego, CA). Calling was by cluster analysis with TYPER 4.0 software (Sequenom). The success rate of genotyping was approximately 99.8 %.

For the confirmatory cohort investigating rs3219487 in the *MUTYH* gene, we used a commercially-available TaqMan SNP genotyping assay (C_110818_10). Genomic DNA was amplified using TaqMan Universal PCR Master Mix (Applied Biosystems, Life Technologies, Carlsbad, CA) and the ABI Prism 7300 sequence detection system (Applied Biosystems) according to the manufacturer's instructions. Analysis of the results was done using SDS Software version 1.3 (Applied Biosystems). Genotyping data were acquired by a researcher blinded to all clinical information.

TaqMan Real-Time Quantitative RT-PCR Assay

Total RNA was isolated from each sample of peripheral mononuclear cells and liver using RNeasy Mini Kit (QIAGEN GmbH, Hilden, Germany). The primers were *MUTYH* (Hs01014856_m1) and 18S ribosomal RNA(Hs03928985_g1). Forty ng of each RNA was applied for reverse transcription and amplification according to the manufacturer's protocol. *MUTYH* mRNA and 18S ribosomal RNA were reverse transcribed at 60˚C for 30 minutes, followed by a PCR cycle with a melting step for 20 seconds at 94˚C and annealing for 1 minute at 60˚C for a total of 40 cycles using the ABI PRISM 7300 Sequence Detection System (Applied Biosystems). The parameter Ct is defined as the fractional cycle number at which the fluorescence generated by cleavage of the probe passes a fixed threshold above baseline. The

standard curve was constructed with 4-fold serial dilutions of total RNA from human peripheral mononuclear cells (calibrator) and composed of five points (400, 100, 25, 6.2, and 1.6 ng total RNA). The *MUTYH* and 18S ribosomal RNA relative to the calibrator, termed [*MUTYH*] c and [18S rRNA] c, respectively, in unknown samples, was quantified by measuring Ct and using a standard curve to determine the starting target message quantity. The final relative *MUTYH* mRNA level was expressed as follows: Relative *MUTYH* mRNA level=[*MUTYH*] c / [18S rRNA] c.

We performed duplicate experiments for each data point. Each RT-PCR run included the five points of the standard curve, a no-template control, the calibrator total RNA, and 40 unknown total RNAs. All of the samples with a coefficient of variation for relative messages to the calibrator data>10% were retested, according to a previous report[24].

Cell Culture

Human hepatoma cell lines Huh-7 and HepG2 were obtained from American Type Culture Collection (ATCC, Manassas, VA). They were cultured in complete Dulbecco's modified Eagle´s medium (Invitrogen, Carlsbad, CA) containing 10% fetal calf serum (Flow Laboratories, North Ryde, Australia) in tissue-culture flasks; incubation was at 37˚C in an atmosphere of air containing 5% CO_2.

Luciferase assay

Transfections were performed using Lipofectamine LTX and Plus reagents (Invitrogen) according to the manufacturer's protocol. For dual-luciferase assays, the cells were transiently cotransfected with firefly luciferase reporter constructs together with the pGL4.75 vector (Promega) containing the Renilla luciferase gene for internal normalization. Intron 6 of *MUTYH* (Major allele sequence (IVS6+35G);

5’-gtgagagccaccctagggtaggggaaataggaacgatagagggactgacgggtgatctctttgacctctgatcctacccacag-3’, minor allele sequence (IVS6+35A); 5’-gtgagagccaccctagggtaggggaaataggaacaatagagggactgacgggtgatctctttgacctctgatcctac ccacag-3’) was inserted into the multicloning site of the pGL4.10 vector (Promega) and designated pIVS6+35G and pIVS6+35A. Fragments of the *MUTYH* promoter (-2000 to +200 and -1000 to +200) were prepared by PCR. The oligonucleotide 5'-AACTCGAGGGGAATTTACCGATGCCCAGAACG-3' (position +177 to +200 with XhoI linker) was used as the downstream primer for all reactions. Each of the following oligonucleotides (with KpnI linker) was used as an upstream primer to amplify specific deletion fragments: 5'-GAGGTACCATGTTCACCCTGGGAGAAAGAGAAGTC-3' (-2000 to -1974) for p-2KB+IVS6+35G and p-2KB+IVS6+35A, and 5'-GAGGTACCCCCACAAGCCTTTGTAACCCACGTGTT-3' (-1000 to -974) for p-1KB+IVS6+35G and p-1KB+IVS6+35A. The amplified fragments were then subcloned into XhoI/KpnI-digested pIVS6+35G and pIVS6+35A. Promoter activities were measured by a Dual Luciferase Reporter Assay System (Promega) and an LD 400 luminometer (Beckman Coulter, Brea, CA). Each experiment was independently repeated six times and each sample was run in triplicate.

Mice

MUTYH-null (*Mutyh* -/-) mice established as described[25]. They were backcrossed onto C57BL/6 for at least 10 generations, yielding 36 wild-type, 51 heterozygous and 51 MUTYH-null mice. All animals were maintained in an air-conditioned specific pathogen-free room with a time-controlled lighting system. Mice were placed on a standard diet containing 45 mg/kg iron (D12041503, Research Diets Inc., New Brunswick, NJ) or a high-iron diet containing 225 mg/kg iron (D12041503, Research Diets Inc.). N-Acetyl-L-cysteine (NAC)

(0.2% in the diet) (D12041503, Research Diets Inc.) was given to 4-week-old heterozygous and MUTYH-null mice.

At 6 or 12 months of age, all mice were sacrificed and their livers removed and fixed in 4% formaldehyde fixative. The handling and sacrificing of all animals was carried out in accordance with nationally-prescribed guidelines, and ethical approval for the studies was granted by the Animal Care and Use Committee of Sapporo Medical University. Blood was harvested immediately after sacrifice via arterial collection. Complete blood counts and ALT levels were measured at Kishimoto Clinical Laboratory, Inc. (Sapporo, Japan).

Semi-quantitative assessment of tissue iron accumulation (Perl's Prussian blue staining)

Perl's Prussian blue staining is a classic semi-quantitative method to assess iron accumulation within tissues. Here, we assessed iron accumulation in liver tissue using criteria previously published by Rowe et al[26]. Briefly, Grade 0 was assigned if granules were absent or barely discernible at 40x magnification; Grade 1, if barely discernible at 20x; Grade 2 if granules were seen at 10x; Grade 3 if granules were seen at 2x; and Grade 4 if granules could be seen with the naked eye.

Hepatic iron concentration

For sample preparation, tissue was dried at 120°C for 24 hours, homogenized and digested using nitric acid and sulphuric acid (1.0 mL of 1 N HNO_3 and 1.0 mL of 1 N H_2SO_4 per 0.1 g dry tissue) while heating. After dilution with de-ionized water (9.0 mL de-ionized water per 1.0 mL of 1 N HNO_3) and centrifugation at 3000 rpm for 10 min, iron levels were determined using an atomic absorption spectrometer (AAnalyst 800, Perkin Elmer, Norwalk, CT)[27].

8-oxo-7,8-dihydro-2'-deoxyguanosine (8-oxodGuo)

Immunohistochemical analysis of formalin-fixed, paraffin-embedded tissue samples was performed using an avidin-biotin–peroxidase complex technique after microwave antigen retrieval, as described previously[6,28]. Sections (thickness 4 μm) were successively treated with blocking solution, 1 μg/mL anti-8-oxodGuo monoclonal antibody (MOG-020P, Japan Institute for the Control of Aging, Fukuroi, Japan), or normal mouse immunoglobulin G (IgG; Dako, Glostrup, Denmark), biotinylated secondary antibody, and a peroxidase–avidin complex (Envision Plus kit; Dako Japan Co. Ltd, Kyoto, Japan). To obtain excellent signal intensities and clean background, we used Mouse-on-Mouse Polymer IHC Kit (Abcam, Cambridge, UK) for blocking tissue.

The intensity of 8-oxodGuo immunostaining in the sections was assessed using an AxioCam photomicroscope and KS-400 image analyzing system (Carl Zeiss Vision GmbH, Hallbergmoos, Germany). A microscopic image of each liver section was imported into the KS-400 system, and brown-stained tissues, which represent positively stained nuclei of hepatocytes corresponding to 8-oxodGuo immunoreactivity, were converted into a 255-graded gray scale. The average gray scale intensity of each sample was calculated by using the KS-400 image analyzing program and is presented as the ratio relative to each sequential section immunostained by normal mouse IgG. At least three periportal and three perivenous zones were examined in each section, and the average of the scores was calculated.

Immunohistochemical determination of AFP

Sections were successively treated with blocking solution, 8 μg/mL goat anti-AFP primary polyclonal antibody (Santa Cruz Biotechnology, Inc. Santa Cruz, CA), biotinylated secondary antibody, and a peroxidase-avidin complex (Envision Plus kit; Dako Japan Co. Ltd, Kyoto, Japan).

Statistical Analysis

All statistical analyses were performed by JMP 13.0 software (SAS, Cary, NC). Nonparametric procedures, including the Mann-Whitney U test and Chi-square method, were employed for the analysis of baseline characteristics and clinical samples. *In vitro* samples were analyzed using Student's *t*-test. We performed uni- and multivariable logistic regression analyses to assess the association between *MUTYH* genotype and incidence of HCC. Cox proportional hazard regression analysis to determine the hazard ratio (HR) for HCC based on *MUTYH* genotype was performed to assess the risk factor level for HCC development. Variables with a P value<0.1 on univariate analysis, and gender, were included in multivariate analyses. All statistical tests were two-sided, and $P<0.05$ was considered statistically significant.

Results

MUTYH gene Single Nucleotide Polymorphisms and Risk of HCC

In the first exploratory study, logistic regression analyses were used to examine the association between 19 SNPs of *MUTYH*, *OGG1* and *MTH1* genes in subjects developing HCC (n=20) compared to those with chronic hepatitis C but no HCC (CHC, n=20). The results demonstrated significant differences between HCC cases and CHC for only one of these SNPs (rs3219487) in the *MUTYH* gene (Supplemental Table 1). The G/A genotype was associated with higher risk of HCC development than the G/G genotype (OR, 10.231; 95% CI, 1.12-93.3; *P*=0.013).

A confirmatory second phase study was performed for rs3219487. The characteristics of the 93 subjects studied are shown in Supplementary Table 2. HCC developed in 38 of these subjects, with a mean age of 74 years; 52.6% were male. We found that subjects in whom HCC developed were older and had lower platelet counts compared to those who remained free of HCC. The data again showed that increased frequency of A/A or G/A was associated with a higher risk for HCC than G/G (OR, 2.52×10^7; 95% CI, 2.47-; *P*=0.0085 and OR, 7.53; 95% CI, 2.37-29.2; *P*=0.0004, respectively) in a logistic regression model (Table 1). Similarly, older age and lower platelet counts were associated with a significant risk of developing HCC (Supplementary Table 3); therefore, we conducted a multiple classification analysis for these factors using a logistic regression model, because the factors older age and A carrier were extracted as independent risk factors for development of HCC (Table 2).

In the subgroup of patients with a known duration of CHC since diagnosis, 10-year cumulative incidence of HCC among A carriers was 38.0%, compared with 17.6% among genotype G/G carriers (Supplementary Fig. 1). In a Cox proportional hazards regression model, variables with a *P* value<0.1 on univatiate analysis were found to be age, platelet count and *MUTYH* genotype (Supplementary Table 4). After adjusting for gender, age and platelet count

on multivariate analysis, subjects with genotype G/A or A/A had a significantly increased risk of HCC relative to subjects with genotype G/G (HR, 2.52; 95% CI,1.22-5.05) (Supplementary Table 5).

Association of MUTYH mRNA Expression with MUTYH genotype

In order to evaluate the functional effects of the intronic mutations, *MUTYH* mRNA levels in peripheral mononuclear cells and liver tissues were quantified by TaqMan RT-PCR (Fig. 1). The mean relative *MUTYH* mRNA level of peripheral mononuclear cells was 0.54 (0.15-1.64) in subjects with genotype G/G and 0.33 (0.05-0.89) in subjects with genotype G/A or A/A. The mean relative *MUTYH* mRNA level of liver tissues was 0.28 (0.15-1.34) in subjects with genotype G/G and 0.14 (0.10-0.27) in subjects with genotype G/A or A/A. Both the *MUTYH* mRNA levels of peripheral mononuclear cells and liver tissues were significantly lower in subjects with genotype G/A or A/A than in subjects with genotype G/G (P=0.0157 and 0.0108, respectively). These results indicate that subjects with *MUTYH* genotype G/A or A/A may have a higher risk for HCC due to lower expression of *MUTYH*.

Effect of modification of Intronic Variants on transfection activity

To determine whether the decrement of *MUTYH* mRNA in subjects with genotype G/A or A/A is due to differences in transcriptional activity, luciferase reporter genes with fragments of the *MUTYH* promoter (-2000 to +200 or -1000 to +200) and major or minor allele sequences of intron 6 were transfected into Huh-7 and HepG2 cells, and their relative luciferase activities were quantified. All transfections were performed in triplicate, and the results of six determinations for each construct are illustrated in Fig. 2. p-2KB+IVS6+35G, containing a major allele sequence of rs3219487, was more active than p-2KB+IVS6+35A containing only a minor allele sequence of rs3219487, in both Huh-7 and HepG2 cells (2.7-

and 2.3- fold, respectively). p-1KB+IVS6+35G was almost equally as active as p-1KB+IVS6+35A (data not shown). These results indicate that -2000 in the *MUTYH* promoter region, but not -1000 in the *MUTYH* promoter region, is involved in enhanced expression of *MUTYH* by insertion of a major allele sequence of rs3219487.

Liver injury due to a high-iron diet in mice

To clarify the effect of MUTYH activity on liver carcinogenicity under oxidative stress, changes in MUTYH-null (*Mutyh* -/-) mice given a high-iron diet were studied over time. Mild liver fat accumulation and infiltration of inflammatory cells was seen in the liver tissue at 6 months on the high-iron diet, increasing at 12 months (Fig. 3A). Serum ALT levels showed an upward trend in the high-iron group at 6 months relative to controls (Fig. 3B) which became significant at 12 months (Fig. 3C; *Mutyh* +/+ high-iron diet group versus *Mutyh* -/- control diet group, P=0.0315; *Mutyh* +/- high-iron diet group versus *Mutyh* -/- control diet group, P=0.0175; *Mutyh* -/- high-iron diet group versus *Mutyh* +/- control diet group, P=0.0001; *Mutyh* -/- high-iron diet group versus *Mutyh* +/+ control diet group, and *Mutyh* -/- control diet group, P<0.0001). No significant differences were observed among the genotypes. Iron deposition in all animals in the high-iron diet group was confirmed by Perl's Prussian blue staining of the liver tissue after 12 months (Fig. 3D, E). The weight of iron in the liver also increased significantly in the high-iron diet group (Fig. 3F).

Hepatocarcinogenesis on a high-iron diet in* MUTYH-*null mice

No liver tumors were observed in any of the mice after 6 months´ on the high iron diet, but by 12 months, they were present in 4 of 12 *Mutyh* -/- animals (Table 3). All of these liver tumors were large and had multiple foci (Fig. 4A), an increased N/C ratio, and an irregular arrangement of the hepatic cords as observed with HE staining (Fig. 4B). Some parts

of the tumor were associated with fat deposition (Fig. 4C). All tumor sites stained AFP-positive (Fig. 4D), and showed similar pathological findings to human hepatocarcinoma. In contrast, no liver tumors were observed in *Mutyh* +/- and *Mutyh* -/- animals on the the high-iron diet for 12 months provided that the anti-oxidant NAC was also provided in the diet (Table 3).

Accumulation of 8-oxodGuo in the liver of mice on the high-iron diet

Liver tissue 8-oxodGuo staining was performed in order to assess oxidative stress in each group. No significant differences were observed after 6 months dietary intervention (data not shown), but the intensity of 8-oxodGuo staining was significantly increased after 12 months relative to controls (Fig. 4E, F).

Discussion

The aim of the present study was to examine the relationship and causality between gene variants of base excision repair enzymes and human hepatocarcinogenesis. We have previously reported that 8-oxodGuo accumulates in the livers of patients with CHC and HCV-related HCC[6]. Furthermore, we have demonstrated that iron reduction therapy reduces this accumulation of 8-oxodGuo in the liver as well as reducing rates of carcinogenic progression[14]. Thus, we hypothesized that variants of these genes of the base excision repair system would be associated with 8-oxodGuo-induced hepatocarcinogenesis. Employing genotyping assays, we first confirmed that subjects with rs3219487 *MUTYH* genotypes G/A or A/A had a higher incidence of HCC than those with genotype G/G. It is well-known that advanced age, male sex, and progression of hepatic fibrosis, amongst other factors, increase the risk of hepatocarcinogenesis[29-31].In addition, we now find that the A allele of rs3219487 in the *MUTYH* gene is also indicated as a risk factor for hepatocaricinogenesis comparable to these established variables. Furthermore, using a Cox proportional hazards regression model, we found that subjects with the genotype G/A or A/A had a significantly increased risk of HCC relative to subjects with genotype G/G after adjustment for gender, age and platelet count on multivariate analysis.

In humans, inherited *MUTYH* variants are associated with colorectal carcinomas[32-34], and deficiencies in GO repair might be a risk factor for lung cancer[35,36]. However, associations of *MUTYH* variants with HCC had not been determined. Nevertheless, as our above-mentioned observations were highly suggestive of causality between the *MUTYH* genotype G/A or A/A and risk of HCC, we performed TaqMan RT-PCR for quantification of *MUTYH* mRNA levels. As shown in Fig. 1, the results indicated increased *MUTYH* mRNA expression of peripheral mononuclear cells and liver tissues in subjects with genotype G/G compared to G/A or A/A. We then extended this study to investigate the mechanism underlying the induction of *MUTYH*

by intron 6 variants. The results of transient transfection assays (Fig. 2) strongly suggested that the major allele sequence of intron 6 increases *MUTYH* expression whereas the minor allele sequence of intron 6 reduces it. Thus, it was clear that there is a causal relationship between *MUTYH* genotype and carcinogenesis in the human liver.

We next examined whether the differences in MUTYH activity were involved in hepatocarcinogenesis induced by oxidative stress using an MUTYH-null mouse model. Although it had been reported that tumors of the small intestine spontaneously developed after 18 months in these animals[25], no HCC was observed. In our study, we adjusted the amount of iron in the diet to 225 mg/kg to result in a moderate level of iron deposition in the liver, similar to that seen in CHC patients[37]. This resulted in oxidative stress in the liver of MUTYH-null mice equivalent to that in CHC patients. This resulted in oxidative stress in the liver of MUTYH-null mice equivalent to that in CHC patients. This in turn resulted in the development of liver tumors in about one-third of the animals within 12 months. Moreover, administration of NAC, an antioxidant known to act directly and/or by increasing intracellular GSH[38], at the same time as iron in the diet, reduced the risk of developing HCC. These results indicated that decreased MUTYH activity contributes to the development of HCC in the presence of continuous oxidative stress due to excess iron in the liver. In addition, these results raised the possibility that therapeutic intervention to decrease oxidative stress may suppress the development of HCC.

Although sustained virologic response (SVR) rates against HCV can be increased by direct-acting antiviral agents, fibrogenesis may still worsen in some cases despite achieiving SVR (12%)[39]. Moreover, HCC may develop even in patients with an SVR[40-42]. This may be a problem especially for the numerous elderly patients. Our study suggests that SNP genotyping may predict the risk of developing HCC in such patients. We propose that in the setting of appropriate screening intervals, stratification of patients for whom antioxidant treatment would

be appropriate could be achieved in this manner.

We have also observed that iron overload in the liver similar to CHC is also present in about half of non-alcoholic steatohepatitis cases, which have been increasing in recent years.[43] The amount of 8-oxodGuo in the liver is also significantly increased in cancer patients[28] .Thus, we plan to evaluate the risk of cancer development in such cases in the near future.

In conclusion, we report that the incidence of HCC is significantly increased in CHC patients because MUTYH activity is decreased due to inhibition of its transcription in rs3219487 A allele carriers of the *MUTYH* gene. Consistent with this, decreased MUTYH activity in a mouse model resulted in the development of HCC in animals with iron-associated chronic oxidative stress in the liver. Importantly, this could be prevented by simultaneous treatment with an antioxidant drug.

1. Alter MJ. The epidemiology of acute and chronic hepatitis C. Clin Liver Dis 1997;1:559–568.

2. Seeff LB. Natural History of Hepatitis C. Hepatology 1997;26:21s–28s.

3. Wasley A, Alter MJ. Epidemiology of Hepatitis C: Geographic Differences and Temporal Trends. Semin Liver Dis 2000;20:1–16.

4. Bassett SE, Bisceglie AMD, Bacon BR, et al. Effects of Iron Loading on Pathogenicity in Hepatitis C Virus–Infected Chimpanzees. Hepatology 1999;29:1884–1892.

5. Hayashi H, Takikawa T, Nishimura N, et al. Improvement of serum aminotransferase levels after phlebotomy in patients with chronic active hepatitis C and excess hepatic iron. Am J Gastroenterol 1994;89:986–988.

6. **Kato J**, Kobune M, Nakamura T, et al. Normalization of Elevated Hepatic 8-Hydroxy-2'-Deoxyguanosine Levels in Chronic Hepatitis C Patients by Phlebotomy and Low Iron Diet. Cancer Res 2001;61:8697–8702.

7. Poli G, Parola M. Oxidative damage and fibrogenesis. Free Radic Biol Med 1997;22:287–305.

8. Kasai H, Nishimura S. Hydroxylation of deoxyguanosine at the C-8 position by ascorbic acid and other reducing agents. Nucleic Acids Res 2006;12:2137–2145.

9. Shibutani S, Takeshita M, Grollman AP. Insertion of specific bases during DNA synthesis past the oxidation damaged base 8-oxodG. Nature 1991;349:431–434.

10. Bonkovsky HL. Iron and the liver. Am J Med Sci 1991;301:32–43.

11. **Kato J**, Kobune M, Kohgo Y, et al. Hepatic iron deprivation prevents spontaneous development of fulminant hepatitis and liver cancer in Long-Evans Cinnamon rats. J Clin Invest 1996;98:923–929.

12. Shimoda R, Nagasima M, Sakamoto M, et al. Increased Formation of Oxidative DNA Damage, 8-Hydroxydeoxyguanosine. Cancer Res 1994;54:3171–3172.

13. Farinati F, Cardin R, Degan P, et al. Oxidative DNA damage in circulating leukocytes occurs as an early event in chronic HCV infection. Free Radic Biol Med 1999;27:1284–1291.

14. **Kato J**, **Miyanishi K**, Kobune M, et al. Long-term phlebotomy with low-iron diet therapy lowers risk of development of hepatocellular carcinoma from chronic hepatitis C. J Gastroenterol 2007;42:830–836.

15. Al-Tassan N, Eisen T, Maynard J, et al. Inherited variants in MYH are unlikely to contribute to the risk of lung carcinoma. Hum Genet 2004;114:207–210.

16. Parker AR, O'Meally RN, Oliver DH, et al. 8-Hydroxyguanosine Repair Is Defective in Some Microsatellite Stable Colorectal Cancer Cells. Cancer Res 2002;62:7230–7233.

17. **Nakabeppu Y**, Tsuchimoto D, Ichinoe A, et al. Biological Significance of the Defense Mechanisms against Oxidative Damage in Nucleic Acids Caused by Reactive Oxygen Species: From Mitochondria to Nuclei. Ann N Y Acad Sci 2004;1011:101–111.

18. Hayakawa H, Hofer A, Thelander L, et al. Metabolic Fate of Oxidized Guanine Ribonucleotides in Mammalian Cells. Biochemistry 1999;38:3610–3614.

19. Yoshimura D, Sakumi K, Ohno M, et al. An Oxidized Purine Nucleoside Triphosphatase, MTH1, Suppresses Cell Death Caused by Oxidative Stress. J Biol Chem 2003;278:37965–37973.

20. Görgens H, Müller A, Krüger S, et al. Analysis of the base excision repair genes MTH1, OGG1 and MUTYH in patients with squamous oral carcinomas. Oral Oncol 2007;43:791–795.

21. Johnson AD, Handsaker RE, Pulit SL, et al. SNAP: a web-based tool for identification and annotation of proxy SNPs using HapMap. Bioinformatics 2008;24:2938–2939.

22. Siva N. 1000 Genomes project. Nat Biotechnol 2008;26:256–256.

23. Gabriel S, Ziaugra L, Tabbaa D. SNP Genotyping Using the Sequenom MassARRAY iPLEX Platform. Curr Protoc Hum Genet 2009;Chapter 2:Unit2.12.

24. **Miyanishi K**, Takayama T, Ohi M, et al. Glutathione S-transferase-π overexpression is closely associated with K-ras mutation during human colon carcinogenesis. Gastroenterology 2001;121:865–874.

25. Sakamoto K, Tominaga Y, Yamauchi K, et al. MUTYH-Null Mice Are Susceptible to Spontaneous and Oxidative Stress Induced Intestinal Tumorigenesis. Cancer Res 2007;67:6599–6604.

26. Rowe JW, Wands JR, Mezey E, et al. Familial hemochromatosis: characteristics of the precirrhotic stage in a large kindred. Medicine (Baltimore) 1977;56:197–211.

27. Sato T, Kobune M, Murase K, et al. Iron chelator deferasirox rescued mice from Fas-induced fulminant hepatitis. Hepatol Res 2011;41:660–667.

28. Tanaka S, **Miyanishi K**, Kobune M, et al. Increased hepatic oxidative DNA damage in patients with nonalcoholic steatohepatitis who develop hepatocellular carcinoma. J Gastroenterol 2013;48:1249–1258.

29. Miki D, Aikata H, Uka K, et al. Clinicopathological features of elderly patients with hepatitis C virus-related hepatocellular carcinoma. J Gastroenterol 2008;43:550–557.

30. Nakagawa H, Maeda S, Yoshida H, et al. Serum IL-6 levels and the risk for hepatocarcinogenesis in chronic hepatitis C patients: An analysis based on gender differences. Int J Cancer 2009;125:2264–2269.

31. Bruix J, Sherman M. Management of hepatocellular carcinoma. Hepatology 2005;42:1208–1236.

32. Al-Tassan N, Chmiel NH, Maynard J, et al. Inherited variants of MYH associated with somatic G:C→T:A mutations in colorectal tumors. Nat Genet 2002;30:227–232.

33. Jones S, Emmerson P, Maynard J, et al. Biallelic germline mutations in MYH predispose to multiple colorectal adenoma and somatic G:C→T:A mutations. Hum Mol Genet 2002;11:2961–2967.

34. Sampson JR, Dolwani S, Jones S, et al. Autosomal recessive colorectal adenomatous polyposis due to inherited mutations of MYH. The Lancet 2003;362:39–41.

35. Xie Y, Yang H, Cunanan C. Deficiencies in Mouse Myh and Ogg1 Result in Tumor Predisposition and G to T Mutations in Codon 12 of the K-Ras Oncogene in Lung Tumors. Cancer Res 2004;64:3096–3102.

36. Zhou P, Li B, Ji J, et al. A systematic review and meta-analysis of the association between OGG1 Ser326Cys polymorphism and cancers. Med Oncol 2015;32:31–16.

37. Furutani T, Hino K, Okuda M, et al. Hepatic Iron Overload Induces Hepatocellular Carcinoma in Transgenic Mice Expressing the Hepatitis C Virus Polyprotein. Gastroenterology 2006;130:2087–2098.

38. Kívia de A, Fabiana M, John DS, et al. Oxidative Stress and Inflammation in Hepatic Diseases: Therapeutic Possibilities of N-Acetylcysteine. Int J Mol Sci 2015;16:30269–30308.

39. Lee YA, Friedman SL. Reversal, maintenance or progression: What happens to the liver after a virologic cure of hepatitis C? Antiviral Res 2014;107:23–30.

40. Yamashita N, Ohho A, Yamasaki A, et al. Hepatocarcinogenesis in chronic hepatitis C patients achieving a sustained virological response to interferon: significance of lifelong periodic cancer screening for improving outcomes. J Gastroenterol 2013;49:1504–1513.

41. Zeng Q, Li B, Zhang X, et al. Clinical Model for Predicting Hepatocellular Carcinomas in Patients with Post-Sustained Virologic Responses of Chronic Hepatitis C: A Case Control Study. Gut Liver 2016;10:955–961.

42. El-Serag HB, Kanwal F, Richardson P, et al. Risk of Hepatocellular Carcinoma After Sustained Virological Response in Veterans With Hepatitis C Virus Infection. Hepatology 2016;63:130–137.

43. Hoki T, **Miyanishi K**, Tanaka S, et al. Increased duodenal iron absorption through up-regulation of divalent metal transporter 1 from enhancement of iron regulatory protein 1 activity in patients with nonalcoholic steatohepatitis. Hepatology 2015;62:751–761.

Author names in bold designate shared co-first authorship.

Figure 1. Relative *MUTYH* mRNA expression in HCV-positive patients.

Relative mRNA expression levels of *MUTYH* were measured by TaqMan real-time PCR. (A) *MUTYH* mRNA levels of peripheral mononuclear cells in subjects with genotype G/G were higher than in genotype G/A or A/A (P = 0.0157, Wilcoxon-Mann-Whitney's U test). (B) *MUTYH* mRNA levels of liver tissues in subjects with genotype G/G were higher than in genotype G/A or A/A (P = 0.0108, Wilcoxon-Mann-Whitney's U test). 18S ribosomal RNA was used as the endogenous control for data normalization. The bottoms and tops of the boxes depict the 25th and 75th percentiles, respectively. Median values are shown by the line within the box. Values outside the top and bottom 95th percentiles are shown individually (closed circles).

Figure 2. Transcriptional regulatory activity of MUTYH in Huh-7 and HepG2 cells.

(A) Huh-7 or (B) HepG2 cells were cotransfected with p-2KB+IVS6+35G or p-2KB+IVS6+35A, and their relative luciferase activities were then determined. p-2KB+IVS6+35G, containing a major allele sequence of rs3219487, was more active than p-2KB+IVS6+35A which contained a minor allele sequence in Huh-7 and HepG2 cells (2.7-fold and 2.3-fold, respectively). Significances of the differences between p-2KB+IVS6+35G and p-2KB+IVS6+35A were determined using the Student's t-test.

Figure 3. A high-iron diet induces a fatty liver, liver injury and accumulations of iron.

(A) Photomicrographs of livers from a control (Cont) or a high-iron diet (Fe) mouse after 6 (a; Cont-*Mutyh* +/+, b; Cont-*Mutyh* +/−, c; Cont-*Mutyh* −/−, d; Fe-*Mutyh* +/+, e; Fe-*Mutyh* +/−, f; Fe-*Mutyh* −/−) or 12 months (g–l) of feeding the high iron diet. Representative liver sections stained with hematoxylin-eosin (H&E). Serum ALT at 6 (B) or 12 (C) months. Data are

expressed as the mean ± SEM for 6-12 mice per group. Representative images of Perl's Prussian blue staining of liver tissue from *Mutyh* –/– mice fed a control (D) or a high-iron diet (E) for 12 months. Strong Prussian blue staining is seen in the cytoplasm of hepatocytes in Fe-*Mutyh* –/– mice. (F) Mice were administered a control diet or a high-iron diet for 12 months. Livers were collected and the iron concentrations were determined by atomic absorption spectrometry as described in "Materials and Methods." The bottoms and tops of the boxes are the 25th and 75th percentiles, respectively. Median values are shown by the line within the box. Values outside the top and bottom 95th percentiles are shown individually. a: $P = 0.0315$ versus Cont-*Mutyh* –/–, b: $P = 0.0175$ versus Cont-*Mutyh* –/–, c $P = 0.0001$ versus Cont-*Mutyh* +/–, $P < 0.0001$ versus Cont-*Mutyh* +/+ and Cont-*Mutyh* –/–, d: $P < 0.05$ versus Cont-*Mutyh* +/+ , Cont-*Mutyh* +/- and Cont-*Mutyh* -/-, e: $P < 0.01$ versus Cont-*Mutyh* +/- and Cont-*Mutyh* -/-, f: $P < 0.05$ versus Cont-*Mutyh* +/- and Cont-*Mutyh* -/-.

Figure 4. *Mutyh* –/– mice fed a high-iron diet develop liver tumors. (A) Gross liver from *Mutyh* –/– mice fed a high-iron diet for 12 months showing multiple tumor foci at the time of necropsy. Representative liver tumor sections stained with hematoxylin-eosin (H&E) (B and C; ×50) and AFP staining (D). (E) Photomicrographs of livers from control (Cont) or high-iron diet (Fe) mice at 12 months (a; Cont-*Mutyh* +/+, b; Cont-*Mutyh* +/–, c; Cont-*Mutyh* –/–, d; Fe-*Mutyh* +/+, e; Fe-*Mutyh* +/–, f; Fe-*Mutyh* –/–). Representative liver sections stained with 8-oxo-7,8-dihydro-2'-deoxyguanosine (8-oxodGuo). (F) Comparison between hepatic 8-oxodGuo levels in mice fed a control or a high-iron diet. The intensity of 8-oxodGuo immunostaining in the sections was assessed using an AxioCam photomicroscope and KS-400 image analyzing system as described in "Materials and Methods." The bottoms and tops of the boxes are the 25th and 75th percentiles, respectively. Median values are shown by the line within the box. Values outside the top and bottom 95th percentiles are shown individually. a :

$P < 0.05$ versus Cont-*Mutyh* +/+ and Cont-*Mutyh* +/-, b : $P < 0.05$ versus Cont-*Mutyh* +/+ , Cont-*Mutyh* +/- and Cont-*Mutyh* -/- .

Table 1. Associations of rs3219487 with HCC Risk

	No HCC		HCC		OR (95%CI)		*P* value
G/G	51	(92.7%)	22	(57.9%)	1		
G/A	4	(7.3%)	13	(34.2%)	7.53	(2.37-29.2)	0.0004
A/A	0	(0.0%)	3	(7.9%)	2.52×10^{7}	(2.47-)	0.0085
A carrier	4	(7.3%)	16	(42.1%)	9.27	(3.01-35.3)	< 0.0001

Table 2. Risk for Development of HCC (multivariate analysis)

	OR	95%CI	*P* value
Age	1.06	1.00-1.13	0.0350
Platelet count	0.93	0.85-1.01	0.1045
rs3219487 , A carrier	9.27	2.39-32.1	0.0005

Table 3. HCC Incidence in mice

Feeding period	Mice			Number of mice	Liver tumor
6 months	Cont	– *Mutyh*	+/+	6	0 / 6
	Cont	– *Mutyh*	+/-	6	0 / 6
	Cont	– *Mutyh*	-/-	6	0 / 6
	Fe	– *Mutyh*	+/+	6	0 / 6
	Fe	– *Mutyh*	+/-	6	0 / 6
	Fe	– *Mutyh*	-/-	6	0 / 6
12 months	Cont	– *Mutyh*	+/+	12	0 /12
	Cont	– *Mutyh*	+/-	12	1 / 12
	Cont	– *Mutyh*	-/-	12	1 / 12
	Fe	– *Mutyh*	+/+	12	0 / 12
	Fe	– *Mutyh*	+/-	12	2 / 12
	Fe	– *Mutyh*	-/-	12	4 / 12
	NAC	– *Mutyh*	+/-	6	0 / 6
	NAC	– *Mutyh*	-/-	6	0 / 6

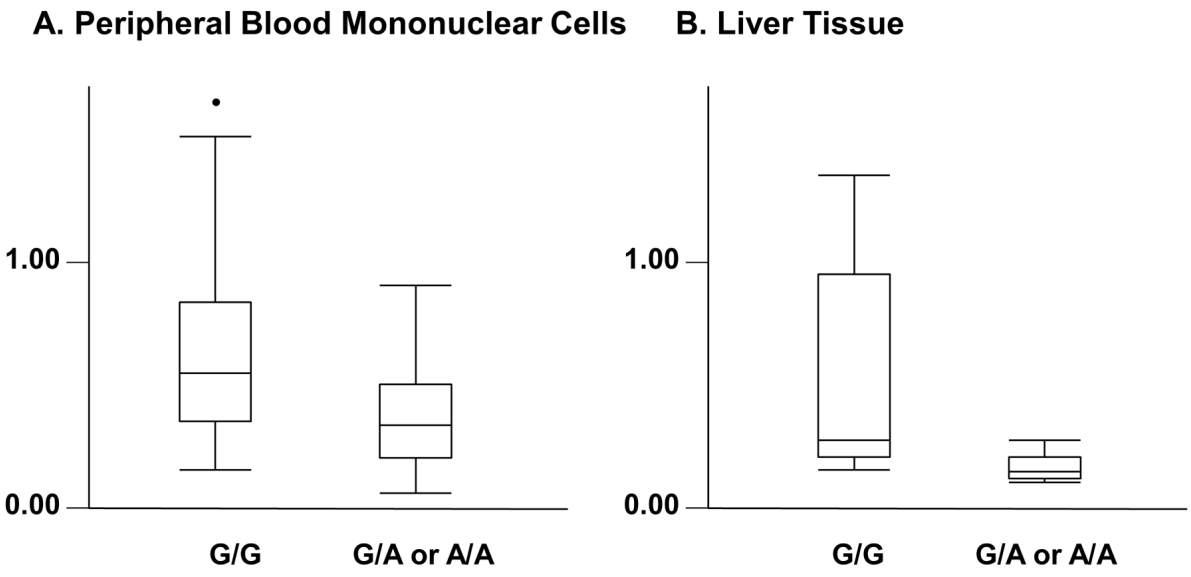
A. Peripheral Blood Mononuclear Cells
B. Liver Tissue
1.00
0.00
G/G
G/A or A/A
1.00
0.00
G/G
G/A or A/A

Figure1

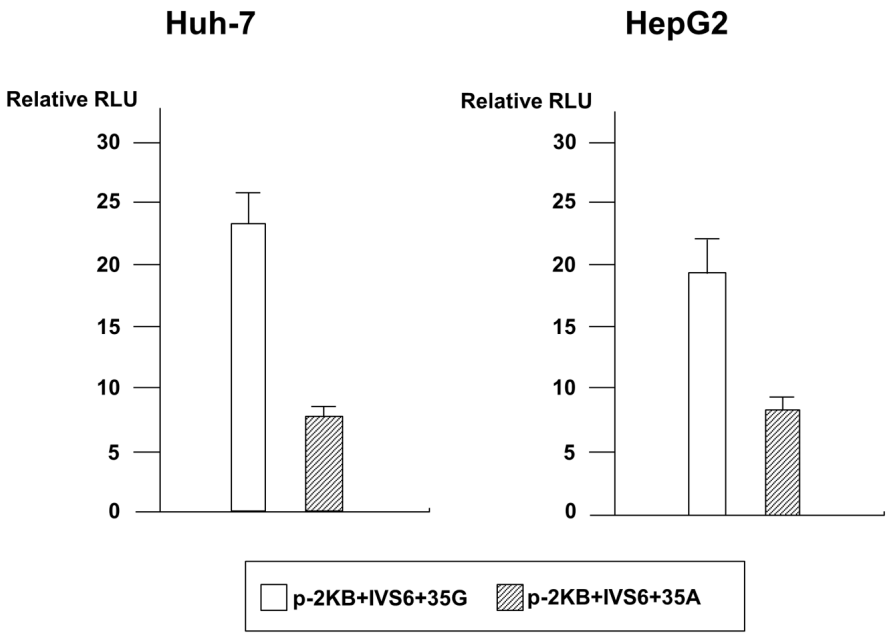
Huh-7
HepG2
Relative RLU
Relative RLU
30
25
20
15
10
5
0
30
25
20
15
10
5
0
p-2KB+IVS6+35G
p-2KB+IVS6+35A

Figure2

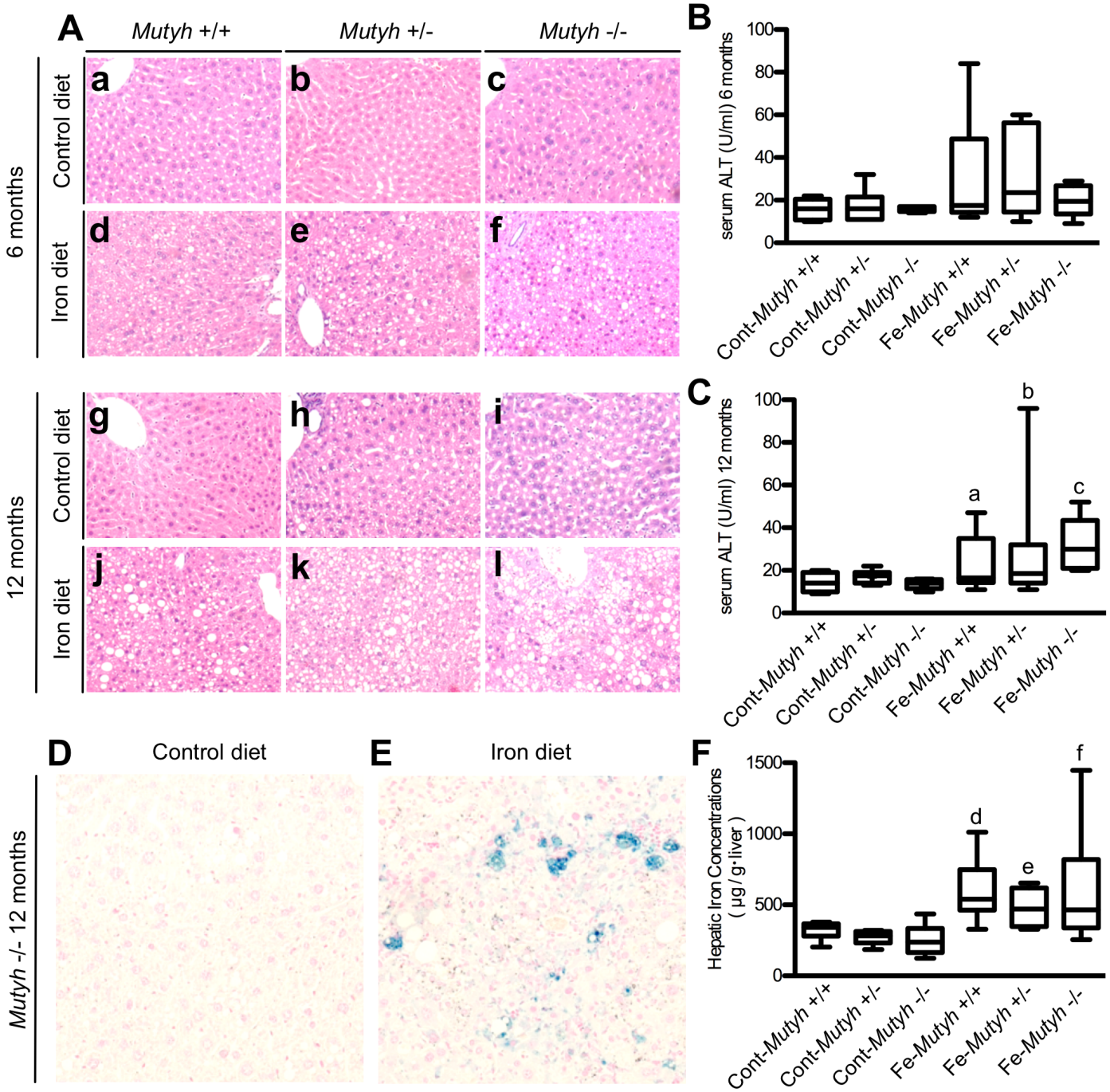
A
Mutyh +/+
Mutyh +/-
Mutyh -/-
6 months
Control diet
Iron diet
a
b
c
d
e
f
12 months
g
h
i
j
k
l
B
serum ALT (U/ml) 6 months
100
80
60
40
20
0
Cont-Mutyh +/+
Cont-Mutyh +/-
Cont-Mutyh -/-
Fe-Mutyh +/+
Fe-Mutyh +/-
Fe-Mutyh -/-
C
serum ALT (U/ml) 12 months
a
b
c
D
Control diet
E
Iron diet
Mutyh -/- 12 months
F
Hepatic Iron Concentrations
(μg / g · liver)
1500
1000
500
0
d
e
f

Figure3

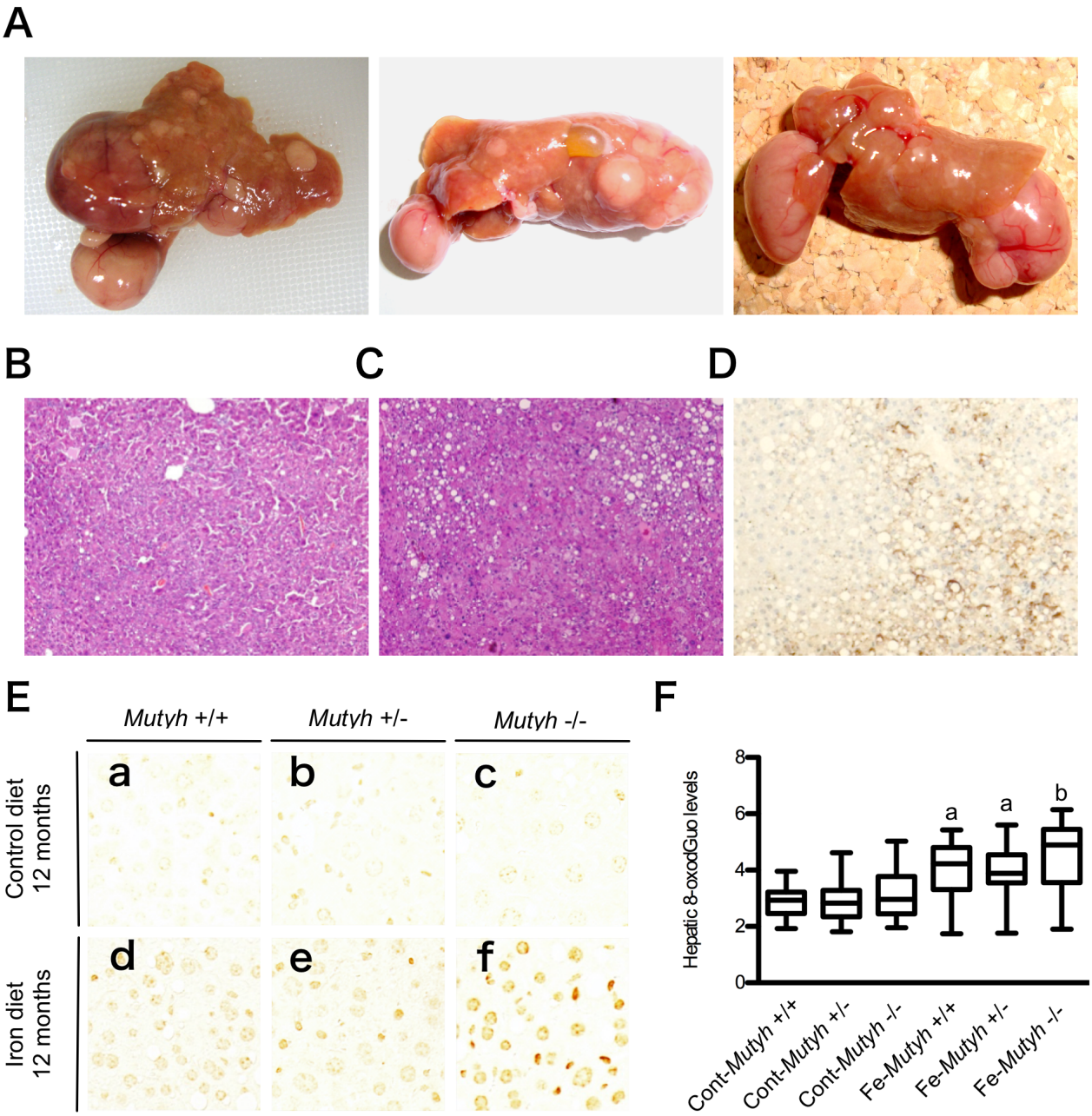
A
B
C
D
E
Mutyh +/+
Mutyh +/-
Mutyh -/-
Control diet
12 months
Iron diet
12 months
a
b
c
d
e
f
F
Hepatic 8-oxodGuo levels
0
2
4
6
8
a
a
b
Cont-Mutyh +/+
Cont-Mutyh +/-
Cont-Mutyh -/-
Fe-Mutyh +/+
Fe-Mutyh +/-
Fe-Mutyh -/-

Figure4

Supplementary Figure 1. Time to developing HCC in HCV-positive patients

rs3219487 in *MUTYH* is associated with hepatitis C virus (HCV) - related hepatocellular carcinoma (HCC). Cumulative incidence of HCC according to rs3219487 genotype. The probability of developing HCC from the time of CHC diagnosis according to rs3219487 genotype was assessed by using cumulative incidence curves, with censoring of data at the date of last follow-up or death. Only patients with a known duration of infection were included in this analysis. Statistics are shown for the multivariable Cox proportional hazards regression model, variables with a *P* value of < 0.1 on univariate analysis, including age, platelet count and *MUTYH* genotype were included. Multivariable statistics for covariables are as follows (male gender was not significant ($P = 0.4378$) and was eliminated from the model): Age: hazard ratio (HR) =1.12 (95% CI = 1.07–1.19), $P < 0.0001$ (univariable $P < 0.0001$); Platelet count: HR = 0.94 (95% CI = 0.87–1.01), $P = 0.0839$ (univariable $P = 0.0470$); rs3219487, A carrier: HR = 2.52 (95% CI = 1.22–5.05), $P = 0.0070$ (univariable $P = 0.0062$).

Supplemental Table 1. Base excision repair gene SNPs and risk of developing HCC

SNP_ID	Genotypes	HCC cases (n = 20)	CHC cases (n = 20)	OR (95% CI)	*P* value
rs2270052	AA	10	7	Reference	
	AG	7	9	0.544 (0.137−2.167)	0.388
	GG	3	4	0.525 (0.088−3.118)	0.478
	AG + GG	10	13	0.538 (0.151−1.917)	0.336
rs3807429	AA	17	13	Reference	
	AG	2	7	0.218 (0.039−1.232)	0.085
	GG	1	0	NC	
	AG + GG	3	7	0.328 (0.071−1.518)	0.140
rs4719468	GG	5	7	Reference	
	GC	6	10	0.840 (0.182−3.880)	0.823
	CC	9	3	4.200 (0.738−23.907)	0.106
	GC + CC	15	13	1.615 (0.412−6.338)	0.489
rs4721505	GG	16	11	Reference	
	GA	3	8	0.258(0.056−1.194)	0.083
	AA	1	1	0.688(0.039−12.200)	0.799
	GA + AA	4	9	0.306 (0.075−1.246)	0.088
rs10232413	CC	15	11	Reference	

	CT	3	9	0.244 (0.053−1.118)	0.069
	TT	1	0	NC	
	CT + TT	4	9	0.326 (0.079−1.337)	0.109
rs10281945	CC	13	14	Reference	
	CA	6	5	1.292 (0.317−5.275)	0.721
	AA	1	1	1.077 (0.061−19.046)	0.960
	CA + AA	7	6	1.256 (0.334−4.733)	0.736
rs33922585	TT	10	7	Reference	
	TC	7	9	0.544 (0.137−2.167)	0.388
	CC	3	4	0.525 (0.088−3.118)	0.478
	TC + CC	10	13	0.538 (0.151−1.917)	0.336
rs3219463	CC	9	8	Reference	
	CT	7	8	0.778 (0.193−3.127)	0.723
	TT	4	4	0.889 (0.165−4.777)	0.891
	CT + TT	11	12	0.815 (0.232−2.860)	0.749
rs3219472	CC	9	8	Reference	
	CT	7	8	0.778 (0.193−3.127)	0.723
	TT	4	4	0.889 (0.165−4.777)	0.891
	CT + TT	11	12	0.815 (0.232−2.860)	0.749
rs3219476	CC	10	11	Reference	
	CA	2	4	1.818 (0.272−12.170)	0.538
	AA	8	5	3.200 (0.419−24.417)	0.262
	CA + AA	10	9	2.250 (0.362−13.971)	0.372
rs3219487	GG	13	19	Reference	
	GA	7	1	10.231(1.121−93.341)	0.013
	AA	0	0	NC	
	GA + AA	7	1	10.231(1.121−93.341)	0.013
rs293796	CC	14	14	Reference	
	CT	5	4	1.250 (0.276−5.653)	0.772
	TT	1	2	0.500 (0.041−6.166)	0.589
	CT + TT	6	6	1.000 (0.259−3.867)	1.000
rs2075747	GG	7	7	Reference	
	GA	10	8	1.250 (0.308−5.072)	0.755
	AA	3	5	0.600 (0.102−3.536)	0.573
	GA + AA	13	13	1.000 (0.273−3.667)	1.000
rs2269112	CC	11	14	Reference	
	CT	8	5	2.036 (0.518−8.000)	0.308
	TT	1	1	1.273 (0.071−22.720)	0.870
	CT + TT	9	6	1.909 (0.520−7.007)	0.326
rs3872715	GG	6	9	Reference	
	GT	10	7	2.143 (0.521−8.814)	0.291
	TT	4	4	1.500 (0.266−8.449)	0.646
	GT + TT	14	11	1.909 (0.520−7.007)	0.326

rs6763347	AA	5	4	Reference	
	AT	9	10	0.720 (0.146−3.544)	0.686
	TT	6	6	0.800 (0.141−4.534)	0.801
	AT + TT	15	16	0.750 (0.169−3.333)	0.705
rs13084184	TT	7	8	Reference	
	TC	9	7	1.469 (0.357−6.054)	0.594
	CC	4	5	0.914 (0.174−4.811)	0.916
	TC + CC	13	12	1.238 (0.343−4.464)	0.744
rs17252807	AA	13	14	Reference	
	AG	6	6	1.077 (0.276−4.197)	0.915
	GG	1	0	NC	
	AG + GG	7	6	1.256 (0.334−4.733)	0.736
rs34127563	TT	13	14	Reference	
	TG	6	6	1.077 (0.276−4.197)	0.915
	GG	1	0	NC	
	TG + GG	7	6	1.256 (0.334−4.733)	0.736

OR, odds ratio; CI, confidence interval; NC, not calculated.

Supplemental Table 2. Baseline Characteristics of Patients

	Non-HCC	HCC	*P* value
Number of patients	55	38	
Gender , M/F	18/37	20/18	0.0549
Median age , y (range)	68 (48-86)	74 (58-86)	0.0445
Ever smoked (%)			0.4854
Smokers	68	72	
Nonsmokers	32	28	
Median ALT level , IU/L	77 (48-265)	87 (42-278)	0.1007
Median GGT level , IU/L	39 (16-192)	50 (15-234)	0.5362
Median Platelet count , x10000/μL (range)	151 (31-300)	101 (40-258)	0.0225

Supplemental Table 3. Risk for Development of HCC (univariate analysis)

	HR	95%CI	*P* value
Gender , M	2.28	0.98-5.42	0.0550
Age	1.06	1.01-1.12	0.0169
Platelet count	0.91	0.84-0.98	0.0179
rs3219487 , A carrier	9.27	3.01-35.3	< 0.0001

Supplemental Table 4. Cox Proportional Hazards Model for Development of HCC (univariate analysis)

	HR	95%CI	*P* value
Gender , M	1.30	0.67-2.51	0.4378
Age at diagnosis of CHC	1.11	1.05-1.16	< 0.0001
Platelet count	0.94	0.88-0.98	0.0470
rs3219487 , A carrier	2.69	1.34-5.22	0.0062

Supplemental Table 5. Cox Proportional Hazards Model for Development of HCC (multivariate analysis)

	HR	95%CI	*P* value
Age	1.12	1.07-1.19	< 0.0001
Platelet count	0.94	0.87-1.01	0.0839
rs3219487 , A carrier	2.52	1.22-5.05	0.0070

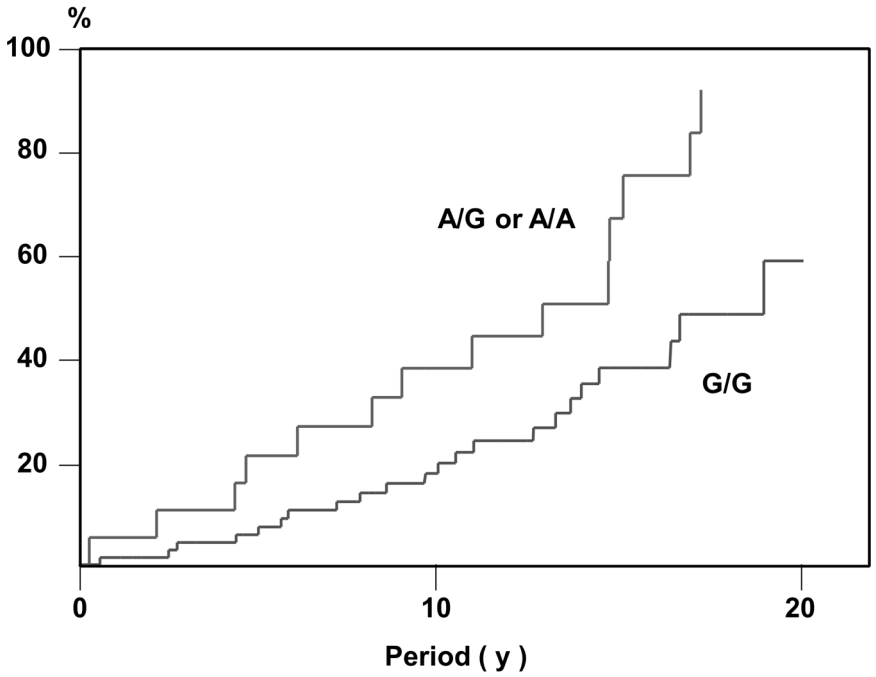

Supplementary Figure1